frontiers in Marine Science

TYPE Original Research
PUBLISHED 02 April 2026
DOI 10.3389/fmars.2026.1805720



OPEN ACCESS

EDITED BY
Alberto Basset,
University of Salento, Italy

REVIEWED BY
Haydee Salmun,
Hunter College (CUNY), United States
Felipe Campos,
Federal University of Pernambuco, Brazil

*CORRESPONDENCE
Angelo Fraga Bernardino
angelo.bernardino@ufes.br

RECEIVED 06 February 2026
REVISED 12 March 2026
ACCEPTED 16 March 2026
PUBLISHED 02 April 2026

CITATION
Pereira AP, Anderson AB, Gaurisas DY and Bernardino AF (2026) Effects of the Amazon River plume in benthic distribution across the Amazon-Guianas shelf.
*Front. Mar. Sci.* 13:1805720.
doi: 10.3389/fmars.2026.1805720



# Effects of the Amazon River plume in benthic distribution across the Amazon-Guianas shelf

Araiene Peres Pereira, Antônio Batista Anderson, Daniela Yepes Gaurisas and Angelo Fraga Bernardino*

Benthic Ecology Group, Department of Oceanography and Ecology, Federal University of Espírito Santo, Vitória, Espírito Santo State, Brazil

The Amazon–Guianas continental shelves form a highly dynamic tropical margin under the influence of the Amazon and Orinoco rivers. Regional circulation and river-derived nutrient inputs influence the delivery of particulate organic carbon (POC) to the continental shelf and may play an important role in structuring benthic ecosystems. Although POC production has previously been associated with river plume dynamics, its effects on shelf benthos remain poorly understood. Here, we investigated this relationship using a time-series analysis of Amazon River discharge at the Óbidos station, 21 years of MODIS-Aqua satellite-derived POC data (2003–2023), and benthic invertebrate occurrence records from the Ocean Biodiversity Information System (OBIS). We quantified plume-driven variability in POC and examined its relationship with regional benthic biogeographic patterns across the Amazon–Guianas shelf. We found persistently elevated POC concentrations north of the Amazon mouth, consistent with plume advection by the North Brazil Current, and identified four shelf sectors with distinct 21-year mean POC regimes (Mouth: 127 $\pm$ 37.7 mg m$^{-3}$; North: 318 $\pm$ 88.9 mg m$^{-3}$; Guianan: 174.8 $\pm$ 42.3 mg m$^{-3}$; Orinoco: 270 $\pm$ 85.1 mg m$^{-3}$). OBIS records comprised 4,541 occurrences across 12 phyla and were dominated by Arthropoda, Cnidaria, Echinodermata, and Mollusca, with clear regional differences in phylum composition. Bray–Curtis/UPGMA clustering separated the Mouth region from northern sectors, indicating a distinct assemblage at the phylum level. Machine-learning importance patterns and ordination of predictor space further suggested region-specific controls, with plume-related signals such as POC and salinity minima being more relevant near the Amazon Mouth and Guiana regions, whereas hydrographic constraints including salinity variability, temperature, and depth were more influential in the North and Orinoco sectors. Together, these results indicate a strong link between river-plume carbon dispersal and broad-scale benthic biogeographic organization across the Amazon–Guianas shelf.

KEYWORDS
**Amazon–Guianas shelf, particulate organic carbon, OBIS, benthic phyla, biogeography, spatial patterns, Amazon River plume**

## 1 Introduction

The Amazon continental shelf represents one of the most productive and dynamic coastal regions on the planet, resulting from the complex interaction between hydrodynamic, climatic, and biogeochemical factors (Nittrouer and DeMaster, 1996). One of the main drivers of this dynamic is the Amazon River, which, as the world's largest river in terms of discharge volume, contributes to approximately 17% of the global freshwater runoff to the oceans (Richey et al., 1986). The Amazon River discharge carries enormous quantities of nutrients, sediments, and organic matter, forming an extensive low-salinity plume that extends from the estuary into the western tropical Atlantic, influencing large-scale marine primary productivity, coastal ecosystems and the carbon cycle (Subramaniam et al., 2008; Coles et al., 2013; Bernardino et al., 2022). Primary production under the influence of the Amazon plume is highly variable in space and time, being modulated by factors such as flow seasonality and larger-scale climate patterns (Smith and DeMaster, 1996; Gouveia et al., 2019). A significant portion of the carbon fixed by photosynthesis is converted to particulate organic carbon (POC), which, in turn, is exported to the seafloor and the magnitude of the POC contributed by the Amazon River is estimated at 10 Tg per year (Richey et al., 1990; Ducklow et al., 2001). In comparison, the Congo River, the second-largest river in the world in terms of discharge and drainage area, contributes approximately 2 Tg of POC per year (Coynel et al., 2005).

This POC then becomes an important food source for benthic organisms, which play crucial ecological roles in nutrient cycling, organic matter decomposition, and maintenance of the functioning of marine ecosystems (Smith et al., 2008). However, although POC production along the Amazon plume is relatively well studied (Subramaniam et al., 2008; Coles et al., 2013), knowledge of benthic diversity in the study area remains incipient and is based on few systematic sampling or analytical efforts (e.g., Aller and Stupakoff, 1996; Lana et al., 1996; Gaurisas and Bernardino, 2023; Bernardino et al., 2023; Klautau et al., 2025); consequently, the link between river discharge, POC production, and its effects on benthic assemblages remains unexplored. The importance of the POC becomes even more evident on the Amazon shelf, where surface concentrations of organic carbon exceed those recorded in other oceanic regions, potentially increasing its influence on the local benthic fauna (Smith et al., 2008). Variations in POC availability significantly influence the biomass, trophic composition, and recruitment patterns of benthic macrofauna (Gooday, 2002; Quintana et al., 2015). Therefore, understanding the drivers of benthic communities in the region is an important step towards spatial management of marine biodiversity and its natural resources in Northern Brazil (Sumida et al., 2020).

Benthic assemblages in this region comprise diverse invertebrate groups, particularly polychaetes, molluscs, crustaceans, and cnidarians, including reef-associated corals and hydroids. Available evidence suggests that their distribution and abundance are structured by gradients in productivity and seafloor habitats on the Amazon shelf (Cordeiro et al., 2015; Gaurisas and Bernardino, 2023; Campos et al., 2024; Klautau et al., 2025; Silva et al., 2025). In this context, we aimed to assess the spatio-temporal variability of particulate organic carbon (POC) across the Amazon–Guianas continental shelves and evaluated how plume-driven gradients relate to benthic fauna distribution. We integrated 21 years (2003–2023) of satellite-derived POC with benthic occurrence records compiled in the Ocean Biodiversity Information System (OBIS) to (i) characterize persistent spatial patterns and interannual variability in POC dispersal, and (ii) test whether regional differences in benthic occurrence structure align with plume-influenced carbon and hydrographic regimes. Given the importance of organic-matter supply in shaping benthic assemblages, we hypothesized that sectors more strongly influenced by Amazon discharge and plume-derived POC would exhibit higher benthic occurrence and distinct community composition, since greater delivery of particulate organic material may increase food availability at the seafloor and influence sediment conditions that affect the distribution of benthic taxa. By linking carbon distributions to broad-scale biodiversity patterns, this study advances understanding of river–shelf coupling and the pathways through which large-river plumes may shape benthic biogeography on tropical continental shelves.

# 2 Materials and methods

## 2.1 Study area and datasets

The study area was defined along the Amazon River plume path across the Guiana and Amazonia ecoregions in the North Brazil Shelf province (Spalding et al., 2007). Given the wide latitudinal range and an expected decreasing influence of the river plume northward from the Amazon River mouth, the area was divided into fourteen 1-degree latitude polygons starting at 3°S to 2°S latitude, until 10°N to 11°N latitude (Figure 1). For each polygon, satellite data and descriptive statistics of each variable were extracted. The Amazon River discharge and precipitation data were obtained from the National Hydrometeorological Network (RHN) database available through the ANA (National Water Agency) website (https://www.snirh.gov.br/hidroweb/) at the ÓBIDOS station (Figure 1). This dataset was used to identify periods of high and low discharge of the Amazon River to the Atlantic Ocean. The Amazon River discharge data were obtained for a period of 21 years (2003-2023) with daily resolution.

Particulate Organic Carbon (POC; mg.m$^{-3}$) concentration data were obtained through remote sensing products from the MODIS Aqua satellite collections (Moderate Resolution Imaging Spectroradiometer; 4km spatial resolution; monthly temporal resolution) for a period of 21 years (2003-2023). The MODIS product calculates POC concentrations using an algorithm produced by Stramski et al. (2022) and available on the EarthData – NASA website (https://oceancolor.gsfc.nasa.gov/). This algorithm estimates particulate organic carbon (POC) concentration in mg.m$^{-3}$ based on an empirical relationship derived from *in situ* measurements and remotely sensed blue-green reflectance ratios (Rrs) (Stramski et al., 2008). Besides, the algorithm performs well in large open-ocean regions; some studies have used the Stramski et al. (2008) algorithm to quantify POC concentrations in plumes and estuaries, including the Amazon (López et al., 2012; Wang et al., 2011; Utsumi et al., 2025).

OBIS is a global infrastructure for standardized, interoperable marine biodiversity records (De Pooter et al., 2017; Provoost et al.,

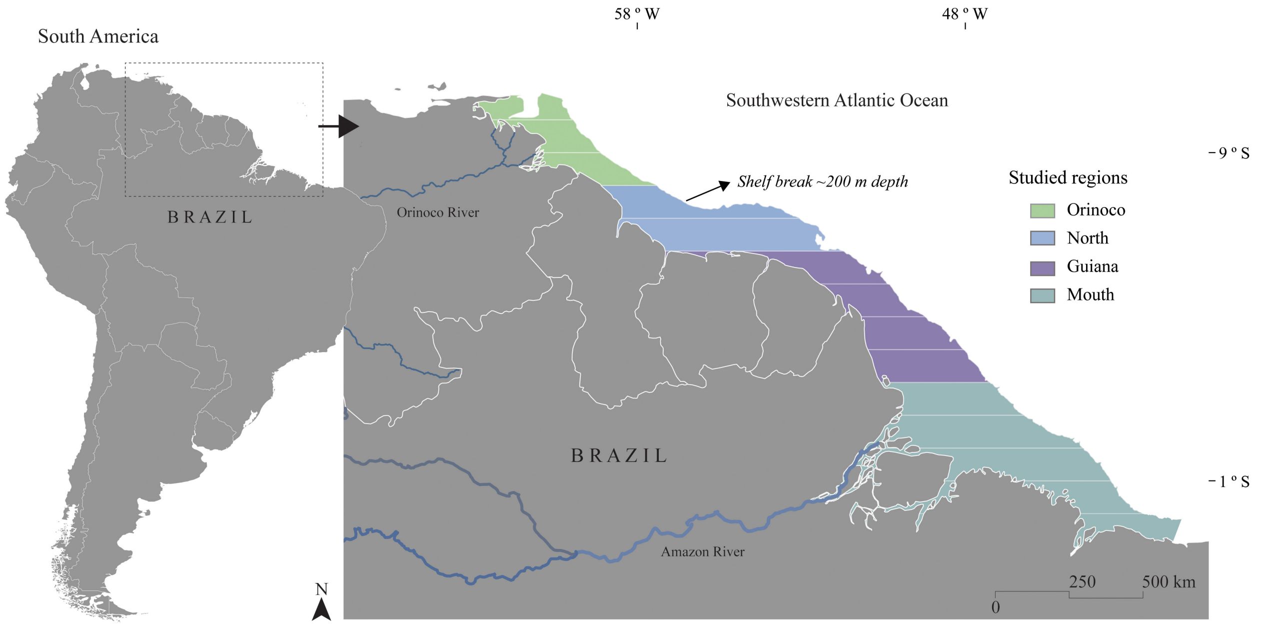


FIGURE 1
Study area map showing the northern South American shelf, the Amazon and Orinoco rivers, the approximate shelf break (~200 m), and the four study regions (Mouth, Guiana, North, and Orinoco).

2017; Vandepitte et al., 2015). Species occurrence data for the study region were obtained from the 'mapper' application on the Ocean Biodiversity Information System (OBIS) website in July 2024, in raster format, and clipped to the four latitude polygons using the 'raster' tool in QGIS 3.32.3 (QGIS Development Team, 2023), using the shapefile of the spatial distribution of species records. Thus, all records distributed outside the polygons were excluded. The clipped occurrence data were manipulated in R-4.3.1 (R Core Team, 2024) to filter benthic invertebrate records according to the functional-group classification available on the World Register of Marine Species website.

## 2.2 Data analysis

The satellite data for POC concentrations were processed in the SeaDAS software (9.1.0 version), which uses algorithms developed by the Ocean Biology Processing Group (OBPG) to calibrate and generate high-precision products. The data generated by the SeaDAS software were then loaded and processed in MATLAB (R2020a version) to obtain mean, median, and total POC concentrations for each month between 2003 and 2023. Annual, decadal, seasonal, and wet/dry period averages were calculated for each latitude range (14 polygons).

The POC values are given in mg.m$^{-3}$ for each pixel in the satellite image, with the respective latitude and longitude values. Thus, the median POC values for each month and polygon were obtained. Median values were used to minimize estimation errors and reduce the influence of extreme values, such as those caused by adjacency effects (Feng and Hu, 2017). To facilitate comparisons and analyses between the latitudes studied, the dissimilarities between latitude polygons were used to create distinct polygon groups through hierarchical agglomerative clustering using the "average" linkage method with Euclidean distance, carried out in software R (version 4.3.1) by using the "cluster" package and visually presented as a dendrogram. To identify potential seasonality and trends, an autocorrelation function (ACF) was computed using the 'stats' package in R (version 4.2.3), with the 'stl' function. The Granger Causality Test was also performed to determine whether one time series can predict another. In this case, the river discharge time series was established as the predictor, and the time series for each polygon group was then tested.

Benthic occurrence records were assigned to their respective polygons and plotted using QGIS 3.32.3 (QGIS Development Team, 2023). Species occurrence maps by phylum in each polygon were produced using the same software. Stacked bar graphs with percentages were plotted using R (version 4.2.3) to observe the prevalence of each phylum and class in each of the defined polygon groups. At the species level, unidentified records (represented by empty fields or containing only commas) were filled in using the genus level, followed by the notation 'sp' (e.g., Genus sp), preserving the taxonomic structure of the sample. Species occurrence records were then transformed to presence/absence to reduce biases in sampling methods and effort between regions. Because OBIS records are spatially heterogeneous, analyses emphasized broad regional and phylum/class-level patterns rather than fine-scale richness comparisons. The occurrence dataset spans records from 0 to 697 m depth, but sampling was concentrated on the inner-to-mid shelf, with 50.8% of records shallower than 50 m and 90.4% shallower than 100 m. Accordingly, interpretations of benthic–environment relationships chiefly reflect shelf habitats within the best-sampled upper 100 m. To help contextualize sampling heterogeneity, the number of source datasets per sector, phylum richness, and class richness were compiled as Supplementary Tables S1–S3.

To summarize broad-scale patterns in regional taxonomic reporting, we produced a cluster heatmap combining a hierarchical dendrogram with a phylum-by-region matrix. Occurrence records were retrieved from the Ocean Biodiversity Information System (OBIS) and aggregated by region and phylum prior to visualization (Zhang and Grassle, 2002). For each region, the number of records per phylum was converted to a percentage of the regional total ["Records (%)"], yielding a compositional matrix suitable for ecological dissimilarity analysis. Pairwise dissimilarities among regions were calculated using the Bray–Curtis dissimilarity (Bray and Curtis, 1957), a standard measure of community (or composition) differences widely used in marine assemblage and biodiversity studies (Clarke, 1993).

Regions were hierarchically clustered using average linkage (UPGMA), producing an "average UPGMA (Bray-Curtis distance)" dendrogram. Cluster robustness was assessed using multiscale bootstrap resampling as implemented in pvclust, which provides bootstrap probability (BP) and approximately unbiased (AU) support values for each internal node (Suzuki and Shimodaira, 2006). The heatmap was constructed from the same phylum-by-region matrix, displayed as tiled cells whose fill colour encodes "Records (%)". Cluster heatmaps are established visual tools that jointly convey matrix structure and hierarchical clustering results (Wilkinson and Friendly, 2009). Graphics were produced in R (R Core Team, 2024) using ggplot2 for layered plotting (Wickham, 2011), with viridis colour maps to ensure perceptual uniformity and colour-vision accessibility (Garnier et al., 2024). Scale transformations and legend formatting were handled with scales (Wickham et al., 2025). To contextualize sampling effort, the total number of OBIS occurrences per region was mapped to circle size and plotted alongside the dendrogram.

## 2.3 Machine-learning analyses

To ensure comparability across regions and taxonomic groups, the dataset was restricted to the seven focal phyla (Echinodermata, Cnidaria, Annelida, Arthropoda, Mollusca, Porifera, and Chordata). The response variable was phylum richness calculated at the sampling-unit scale defined by unique combinations of region, longitude, latitude and occurrence identifier (region × lon × lat × occ). For each sampling unit, phylum richness was computed as the number of distinct phyla present, and predictor variables (POC, temperature minimum/maximum, salinity minimum/maximum) were aggregated by their mean values. Sampling units with missing predictor values were excluded prior to model fitting. Environmental covariates included particulate organic carbon (POC) and Bio-ORACLE-derived minimum/maximum temperature and salinity layers (Assis et al., 2018).

To assess the importance/influence of predictor variables (i.e., POC, salinity, temperature, and depth) on the study area's diversity, a machine learning Random Forest model (RF) was applied. Phylum richness was modelled separately for each region using the Random Forest regression (Breiman, 2001) as implemented in the ranger engine (Wright and Ziegler, 2017). Models were trained using a standardized preprocessing recipe (median imputation, zero-variance filtering, and z-score normalization of predictors) followed by regional v-fold cross-validation. The number of folds was set adaptively as v = min [5, max (2, n − 1)] to avoid invalid resampling configurations in small regional subsets. Hyperparameters were tuned via a regular grid search over mtry (1 to p predictors) and min_n (3 to 25), keeping 1000 trees fixed. The best configuration per region was selected by minimizing cross-validated RMSE; $R^2$ and MAE were also reported. Cross-validation was used for model selection and performance estimation following established methodology (Arlot and Celisse, 2010) and modern applied guidance for predictive modelling workflows (Kuhn and Johnson, 2019). Random Forests were fitted using the ranger implementation (Wright and Ziegler, 2017).

Predictor contributions were quantified using permutation importance from ranger, normalized within the region to facilitate comparisons among predictors. Because variable-importance measures can be sensitive to predictor properties and correlation structure, interpretation focused on within-region relative patterns rather than absolute magnitudes (Strobl et al., 2007; Molnar, 2022). Marginal effects were explored via partial dependence profiles (Friedman, 2001) for the two most influential predictors per region, implemented with the pdp package (Greenwell, 2017). To complement partial dependence with more recent interpretability concepts, we also considered accumulated local effects (ALE) as a theoretical alternative that is less sensitive to extrapolation in correlated-feature spaces (Apley and Zhu, 2020).

## 2.4 Multivariate analysis

To contextualize regional and taxonomic structure in predictor space, a principal component analysis (PCA) was performed on the standardized predictor matrix computed for Region × Phylum centroids (mean predictor values per region and phylum). To summarize whether regions shared similar importance signatures, a region × predictor matrix of within-region normalized permutation importance was built and clustered using hierarchical agglomeration with Euclidean distance and Ward's minimum-variance criterion (Ward, 1963). The resulting dendrogram was used to reorder heatmap rows and to assign regions to k = 3 clusters, which were visualized as colour-coded dendrogram branches alongside the importance heatmap.

# 3 Results

## 3.1 River discharge and POC time series

The time series of the Amazon River discharge at the ÓBIDOS station revealed a biannual oscillation pattern, with discharge increasing during the wet period and decreasing during the dry period (Figure 2). Following the decomposition of the river discharge time series, the seasonal component analysis suggests regular fluctuations that repeat annually with similar patterns and intensity (Figure 2a). Autocorrelation analysis indicates that the discharge of the Amazon River exhibits a seasonal pattern, forming a complete cycle at lag=1, in years, indicating an annual cyclical behaviour on Amazon River's discharge (Figure 2b).

10.3389/fmars.2026.1805720

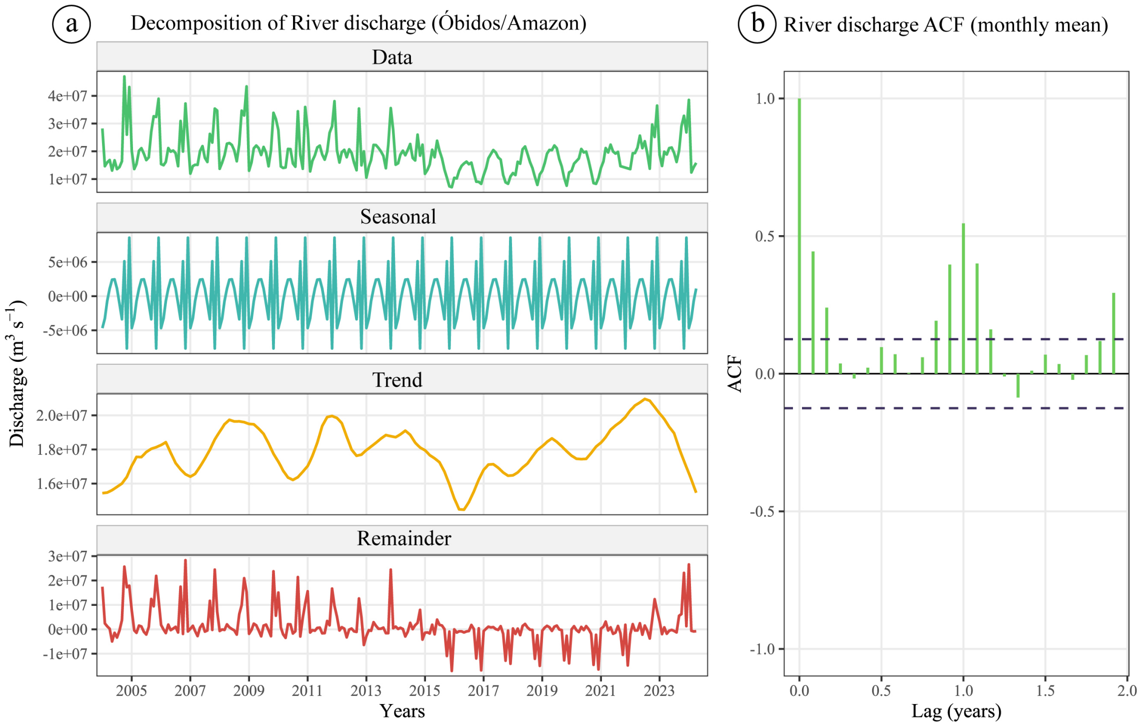


FIGURE 2
Amazon River discharge at Óbidos (2003–2023): **(a)** seasonal–trend decomposition (STL) of monthly mean discharge into observed series (data), seasonal component, long-term trend, and remainder. **(b)** Autocorrelation function (ACF) of the monthly mean discharge; dashed lines indicate approximate 95% confidence limits.

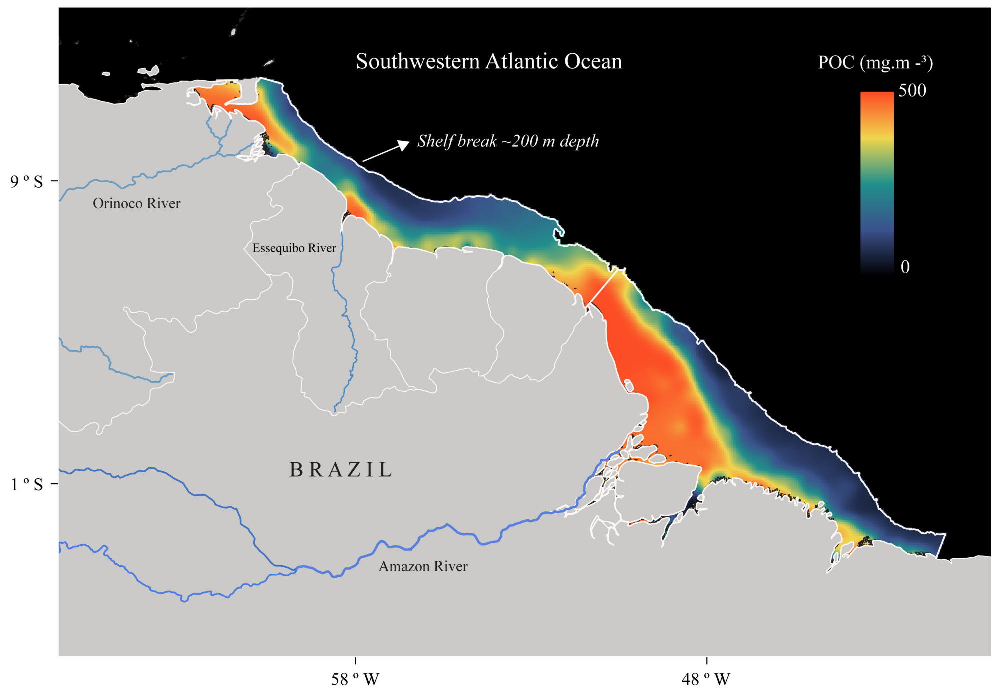


FIGURE 3
Spatial distribution of particulate organic carbon (POC) on the North Brazil Shelf province: map showing the mean POC plume (mg $m^{-3}$) along the Amazon–Guiana margin over the 21-year study period, with major rivers (Amazon, Essequibo, and Orinoco), the approximate shelf break (~200 m), and the main surface plume pathway indicated by the spatial concentration gradient.

The 21-year median surface POC concentration (2003-2023; Figure 3) appears to follow the continental margin. Latitudes closer to the Amazon River mouth, up to 2°N, had the lowest POC concentrations, with values remaining consistently below 150 $mg.m^{-3}$. The 21-year POC concentrations were higher between latitudes 3°N and 6°N, with polygon 8 (4°N–5°N) showing the highest POC concentration (~700 $mg.m^{-3}$). At latitude 6°N, POC concentrations decline until 8°N (120 ± 34.3 $mg.m^{-3}$), then increase again up to latitude 11°N (371.7 ± 98.5 $mg.m^{-3}$). In general, POC concentrations increase from 1°N to 5°N, decline to 8°N, and then rise again towards higher latitudes.

Cluster dissimilarity analysis identified four polygon groups resembling the spatial distribution of POC (Figure 4). From south to north, the first cluster was termed the Mouth Group (Polygons 1–5; 3°S–2°N), with a 21-year mean POC concentration of 127 ± 37.7 mg $m^{-3}$. The second cluster, the North Group (Polygons 6–9; 2°N–6°N), with mean POC of 318 ± 88.9 mg $m^{-3}$. The Guiana Group (Polygons 10–11; 6°N–8°N) presented POC values of 174.8 ± 42.3 mg $m^{-3}$, and the fourth cluster, the Orinoco Group (Polygons 12–14; 8°N–11°N), presented POC values of 270 ± 85.1 mg $m^{-3}$ (Figure 4).

The POC time series for the Guiana and Mouth Groups showed the strongest correlations with river discharge ($p < 0.05$ for both; $r = 0.49$ and $r = 0.46$, respectively), whereas the North and Orinoco Groups exhibited weaker but still significant correlations ($p < 0.05$; $r = 0.28$ and $r = 0.17$, respectively). All groups indicated a causal relationship between river discharge and POC concentrations ($p < 0.05$), with the North and Guiana Groups showing the highest F-statistics ($F = 47.54$ and $F = 43.62$, respectively). Linear regressions between river discharge and POC concentrations also supported stronger model fits for the Guiana and Mouth Groups ($R^2 = 0.24$ and $R^2 = 0.21$, respectively; $p < 0.05$) compared with the North and Orinoco Groups ($R^2 = 0.08$ and $R^2 = 0.03$, respectively; $p < 0.05$).

## 3.2 Benthic records and distribution

OBIS occurrence records were well distributed spatially throughout each study region (Figure 5). A total of 4,541 occurrences from 52 different databases were recorded for the study area after data curation and standardization. Approximately 50.8% of the occurrence data were recorded at depths less than 50 meters, and 90.4% of the occurrences were found within the first 100 meters. Twelve metazoan phyla were found; the phylum with the highest number of occurrences was Arthropoda (1,965 occurrences; 43.3%), followed by Cnidaria (893 occurrences; 19.7%) and Echinodermata (739 occurrences; 16.3%). Mollusca, Annelida, and Porifera also stood out, together comprising 20.0% of total occurrences, while other phyla represented less than 1%. By region, the compiled records were derived from 28 source datasets in the Mouth sector, 24 in North, 17 in Guiana, and 18 in Orinoco, underscoring moderate spatial variation in source coverage.

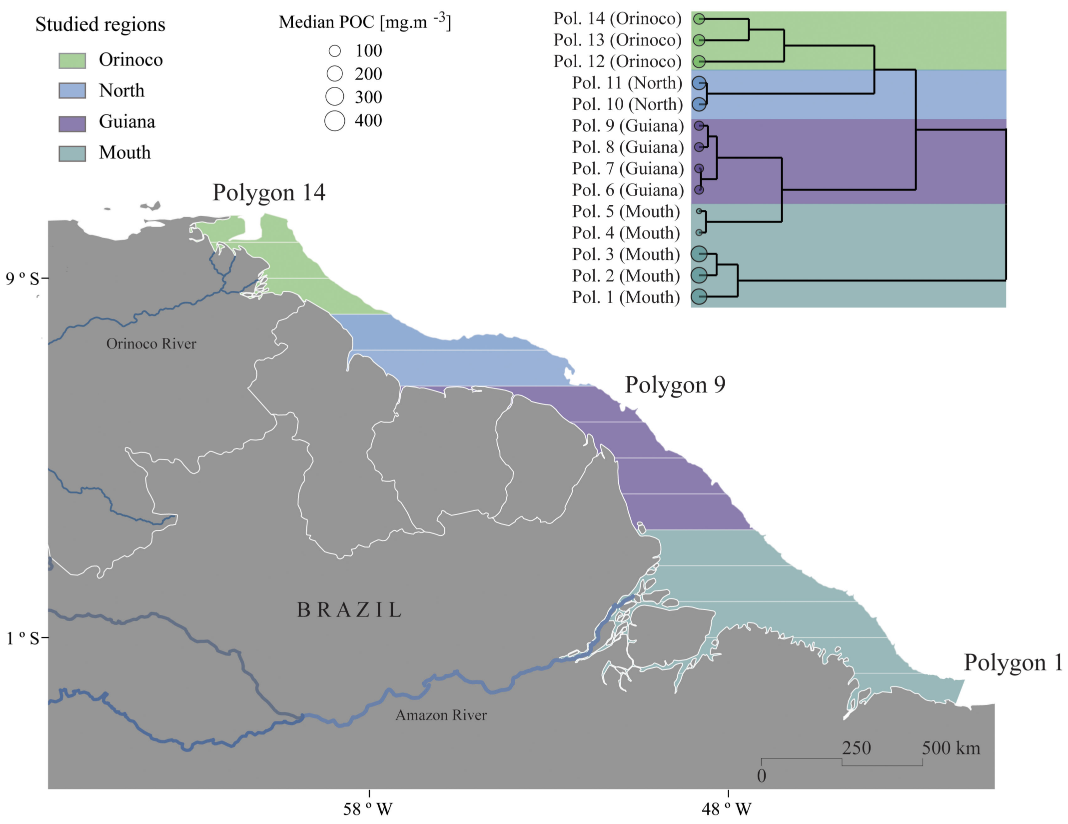


FIGURE 4
Spatial polygons and clustering based on POC across the Amazonia–Guiana shelf: map showing the 14 coastal-shelf polygons grouped into four study regions (Mouth, Guiana, North, and Orinoco). The dendrogram (right) summarizes hierarchical clustering of polygons based on median particulate organic carbon (POC; mg $m^{-3}$), with circle size proportional to polygon median POC and background colours indicating the assigned region.

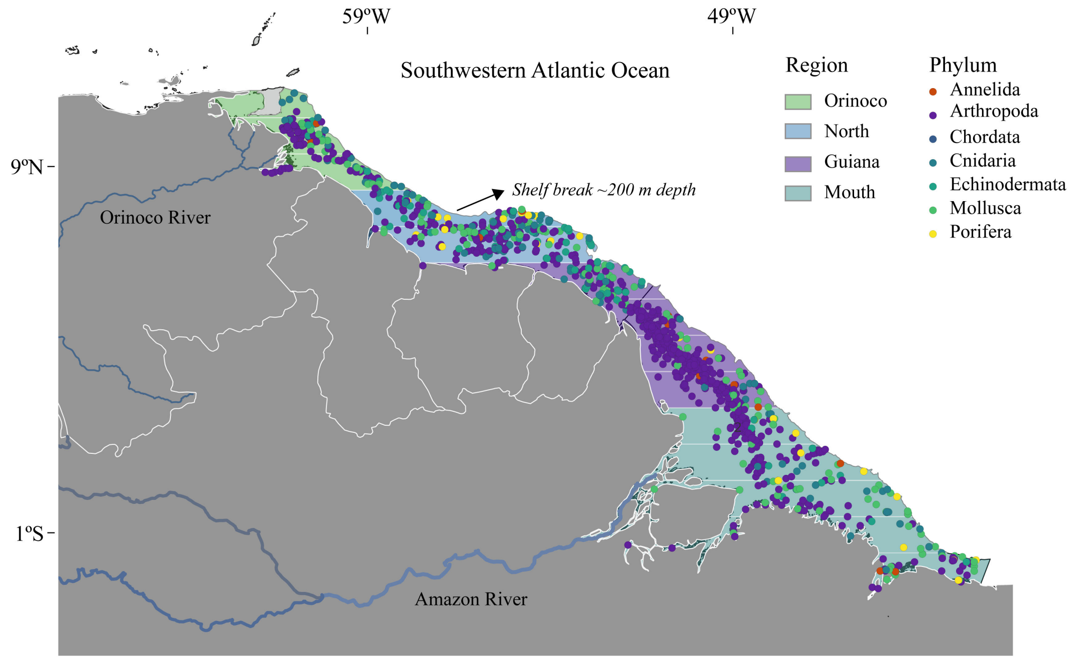


FIGURE 5
Spatial distribution of benthic occurrence records across the Amazonian–Guiana shelf: dots represent georeferenced OBIS occurrence records, and colours identify the seven focal phyla (Annelida, Arthropoda, Chordata, Cnidaria, Echinodermata, Mollusca, and Porifera) along the southwestern Atlantic continental shelf. Shaded polygons delimit the four study regions (Mouth, Guiana, North, and Orinoco); the approximate shelf break (~200 m) and major rivers (Amazon and Orinoco) are indicated.

Most occurrences belonged to the Mouth region (1,271 occurrences; 28.4%), followed by the Orinoco (1,195 occurrences; 25.9%), Guiana (1,069 occurrences; 23.2%), and North (1,006 occurrences; 22.3%) regions. The Guiana and Mouth polygons presented the highest overall species richness, with 241 and 232 species, respectively, whereas the North and Orinoco polygons showed 166 and 201 species. Among the total occurrences for the study region, the predominant classes were Malacostraca (47.0%), Gastropoda (10.4%), Octocorallia (7.3%), Ophiuroidea (6.6%), Asteroidea (6.3%), and Hexacorallia (6.0%). Species richness was not strictly proportional to occurrence frequency: Arthropoda was the most frequent phylum, but regional richness was also high for Cnidaria and Mollusca in the Mouth sector and for Echinodermata in Guiana (Supplementary Tables S2, S3).

Across the Amazonia–Guiana shelf, OBIS benthic occurrence records were dominated by Arthropoda, Cnidaria, and Echinodermata, with secondary contributions from Mollusca, Annelida, Porifera, and Chordata. Regional composition differed markedly. In the Mouth region, Cnidaria represented the largest share of records (38.1%), followed by Arthropoda (35.6%) and Mollusca (15.8%). In contrast, Arthropoda predominated in the North (49.9%), Guiana, and Orinoco regions. In the North region, Mollusca formed the second-largest share (18.8%), followed by Echinodermata (13.4%). Further north, Guiana and Orinoco exhibited elevated relative contributions of Echinodermata (28.6% and 20.3%, respectively), followed by Cnidaria (18.0% and 16.1%). Species-richness summaries showed that Arthropoda had the highest richness in Mouth, North, and Orinoco, whereas Echinodermata reached its greatest richness in Guiana, reinforcing that abundant groups were not always the richest within each sector (Supplementary Table S2).

Arthropods exhibited the highest number of total occurrences (1,965; 43.3%), with Crustacea accounting for the vast majority of these records (99.1%) and Malacostraca being the most frequent class (96.4%) across the four study regions (Figure 6a). Thecostraca was the second most frequent class in the Mouth region (9.3%), while Malacostraca dominated the North, Guiana, and Orinoco regions. Ostracoda was not recorded in the Guiana and Orinoco polygons, whereas Thecostraca was absent from the Orinoco polygon. Ostracoda and Pycnogonida together accounted for less than 1.5% of arthropod occurrences. Arthropoda also showed high species richness, especially in the Mouth and Orinoco sectors, but this pattern should be interpreted cautiously because trawl- and fisheries-derived datasets can disproportionately increase crustacean records. The most representative crustacean species were *Nematopalaemon schmitti*, *Xiphopenaeus kroyeri*, *Meiosquilla schmitti*, and *Pseudosquilla ciliata*.

Cnidaria was the second most abundant phylum in terms of occurrences (893 occurrences; 19.7%). Hydrozoa dominated the Mouth region (51.3%), whereas Anthozoa prevailed in the North, Guiana, and Orinoco regions (>93%), with Octocorallia representing 74.4% of the records in the North region (Figure 6b). Similarly, Octocorallia accounted for 75.0% of the occurrences in the Guiana region, whereas Hexacorallia represented 59.5% in the Orinoco region. The most representative cnidarian species were *Paciforgia elegans, Lytreia plana*, and *Renilla muelleri* (Octocorallia), as well as *Meandrina brasiliensis* and *Madracis pharensis* (Hexacorallia). The contrast between

10.3389/fmars.2026.1805720

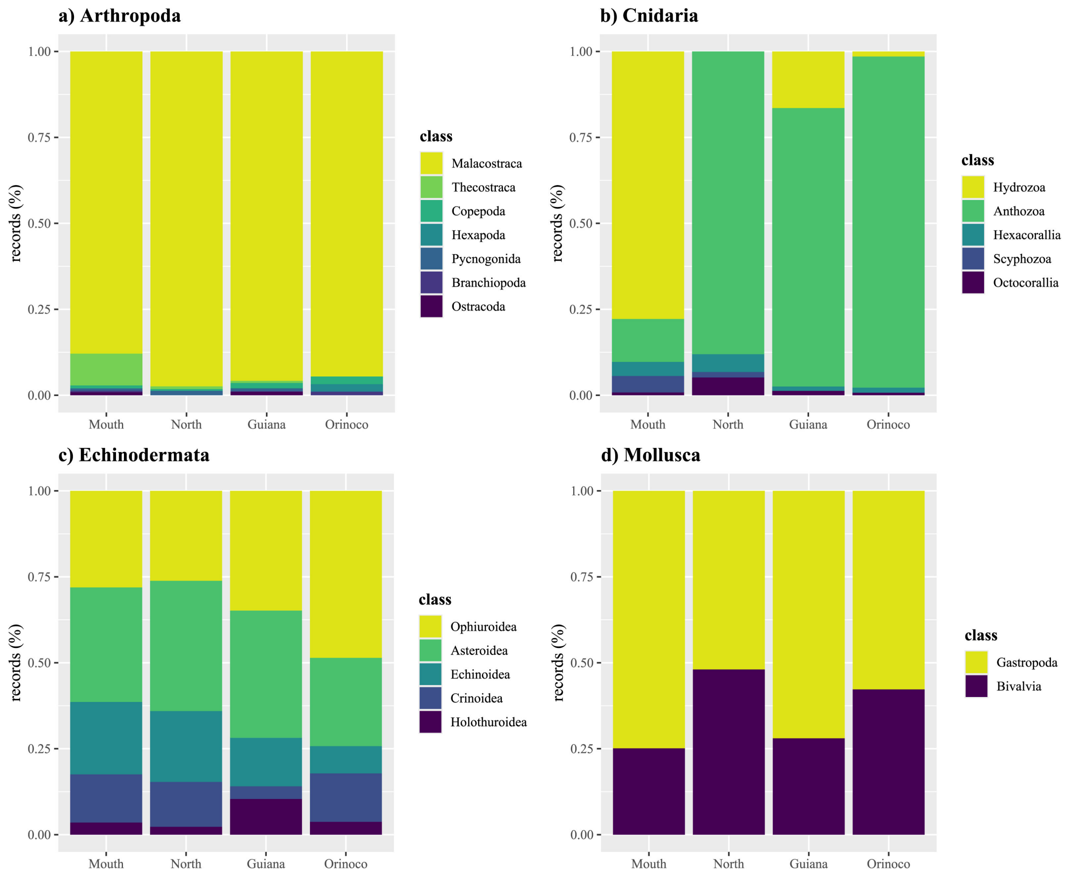


FIGURE 6
Class-level composition of occurrence records by region for selected phyla: stacked bar charts show the proportional contribution of taxonomic classes (records, %) within each study region (Mouth, Guiana, North, and Orinoco) for **(a)** Arthropoda, **(b)** Cnidaria, **(c)** Echinodermata, and **(d)** Mollusca. Colours indicate classes within each phylum.

Hydrozoa dominance near the river mouth and Anthozoa dominance farther north is consistent with differences in substrate availability and habitat type, but it may also partly reflect uneven sampling among sectors. In particular, the Mouth sector includes records associated with consolidated bottoms and reef-related habitats of the Great Amazon Reef System, whereas anthozoan-rich northern sectors include mesophotic and outer-shelf habitats where octocorals and hexacorals are more frequently reported.

The phylum Echinodermata represented the third largest phylum in terms of occurrences (739 occurrences; 16.3%). Within this phylum, Asteroidea (33.4%) and Ophiuroidea (35.2%) were the most frequently recorded classes (Figure 6c). In the Mouth region, the relative contribution of Asteroidea (33.3%) and Ophiuroidea (28.1%) was comparable to that of Echinoidea (21.0%), with additional representation from Crinoidea (14.0%) and Holothuroidea (3.5%). In the North region, occurrences of echinoids (14.5%), sea cucumbers (10.4%), and crinoids (3.7%) were lower than those of starfish and ophiuroids (37.0% and 34.8%, respectively). In the Guiana region, occurrences followed the order Asteroidea (37.9%), Ophiuroidea (26.1%), Echinoidea (20.6%), Crinoidea (13.1%), and Holothuroidea (2.3%). In contrast, the Orinoco region showed a reversed pattern, with Ophiuroidea (48.5%) dominating, followed by Asteroidea (25.7%), Crinoidea (14.1%), Echinoidea (7.9%), and Holothuroidea (3.7%). Echinodermata also reached its highest species richness in Guiana, indicating that regional diversity within this phylum was not captured solely by occurrence totals. The most representative echinoderm species were *Tropiometra carinata, Eucidaris tribuloides*, and *Linckia guildingi*.

Mollusca was the fourth most abundant phylum in occurrences (617 occurrences; 13.6%). Gastropoda dominated occurrences across all regions (66.7%), rivalled only by Bivalvia (Figure 6d). In the Mouth and North regions, Gastropoda accounted for more than 70% of the occurrences, whereas in the Guiana and Orinoco regions its relative contribution ranged between 50% and 60%. Mollusca also maintained comparatively high species richness in Mouth and North, indicating that this phylum contributed both frequent and taxonomically diverse records to the shelf assemblage. The most representative mollusc species were *Polystira albida, Mulinia cleryana*, and *Nassarius scissuratus*.

UPGMA clustering based on Bray–Curtis dissimilarity of phylum composition separated the Mouth region from the remaining regions (Figure 7), indicating that the Mouth assemblage is compositionally distinct at the phylum level. Guiana, North, and Orinoco grouped together despite differences in their secondary phylum contributions, consistent with their shared dominance by Arthropoda. Bubble scaling of regional

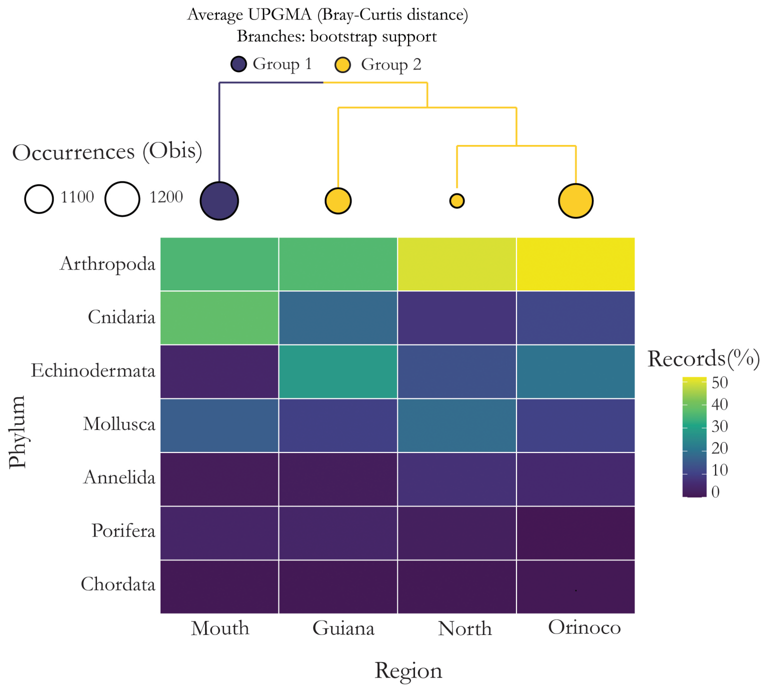


FIGURE 7
Regional composition of OBIS benthic records across the Amazonia–Guiana shelf: heatmap shows the relative contribution of seven focal phyla to occurrence records (%) within each study region (Mouth, Guiana, North, and Orinoco). The dendrogram above summarizes UPGMA clustering (Bray–Curtis distance) of regions based on phylum composition; branch colours indicate the two main clusters, and circle size is proportional to the number of georeferenced occurrence records per region.

record counts further indicates that differences in composition were not simply driven by uneven sampling intensity among regions, although source-dataset heterogeneity remains an important caveat for interpretation.

## 3.3 Environmental drivers of Amazon-Guianas shelf benthos

Random Forest modelling revealed region-specific predictor importance profiles for explaining phylum-level patterns (Figure 8a). In the Guiana region, particulate organic carbon (POC) and salinity (particularly minimum salinity) were among the most influential predictors, whereas the Orinoco region was most strongly associated with salinity variability (especially maximum salinity) and maximum temperature. The Mouth region showed comparatively higher importance for minimum temperature and minimum salinity, while the North region showed a stronger contribution of salinity (minimum/maximum) together with depth. Because permutation importance can be biased under predictor correlation, these patterns should be interpreted in light of known variable-importance properties (Strobl et al., 2007). Hierarchical clustering of the region-by-predictor importance matrix grouped Mouth with North and Guiana with Orinoco (Figure 8a), suggesting two broad regimes of environmental control across the study area.

The PCA ordination of the standardized predictor space across region × phylum observations summarized these gradients (PC1 = 54.1% and PC2 = 26.0% of explained variance; Figure 8b). PC1 primarily contrasted higher salinity and higher maximum temperature against higher POC and lower minimum temperature, while PC2 captured a depth-related gradient. Region ellipses and the distribution of phylum–region observations indicated that Guiana and Mouth tended to occupy the negative side of PC1 (consistent with stronger POC influence), whereas North and Orinoco shifted toward positive PC1 values (consistent with salinity/temperature influence). Together, the RF importance profiles and PCA indicate that phylum-level biogeographic structure across the Amazonia–Guiana shelf is shaped by a spatially varying balance between plume-related POC signals and hydrographic constraints (salinity, temperature, and depth).

# 4 Discussion

The integration of 21 years of satellite-derived particulate organic carbon with Amazon River discharge and OBIS-derived benthic occurrence records revealed that the Amazon River plume discharge structure the shelf benthos across more than 8 degrees of latitude along the Amazon–Guiana margin. Although the effects of large-river plumes on shelf biogeochemistry and organic matter supply along the North Brazil shelf and the Guianas were previously explored (Nittrouer and DeMaster, 1996; Dagg et al., 2004; Coles et al., 2013), this study revealed a marked and previously unknown benthic regionalization linked to plume gradients and POC concentrations. We observed coherent south–north differences in phylum composition and record density, with the Mouth sector standing apart from the Guiana–North–Orinoco sectors. These

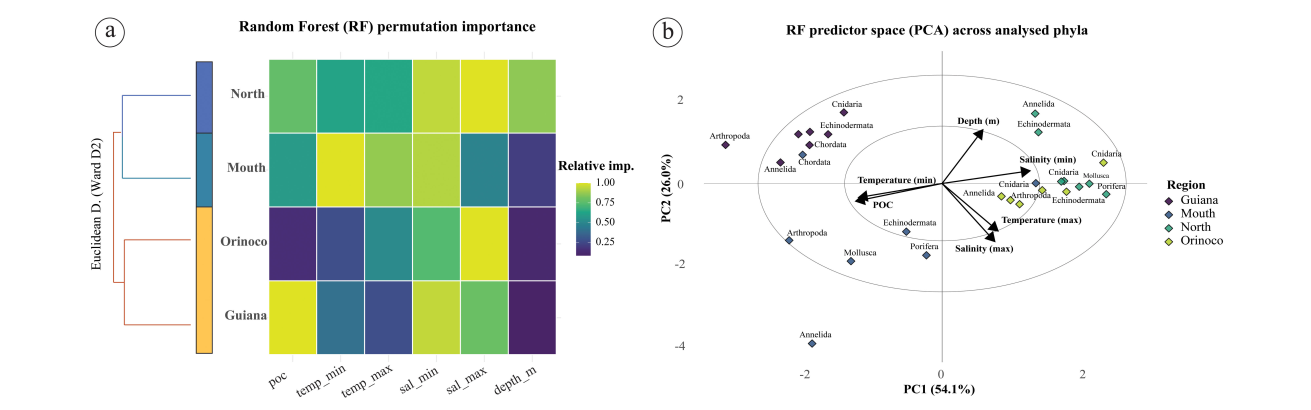


FIGURE 8
Random forest drivers of phylum composition across regions: **(a)** heatmap of random forest (RF) permutation importance (scaled relative importance) for environmental predictors (POC, minimum/maximum temperature, minimum/maximum salinity, and depth) for each study region (Guiana, Orinoco, Mouth and North), with hierarchical clustering of regions based on importance profiles (Euclidean distance; Ward's D2). **(b)** PCA ordination of the RF predictor space across analysed phyla, showing predicto' loadings (arrows) and the distribution of phylum–region observations; ellipses summarize group dispersion by region.

regional differences are consistent with spatial heterogeneity in depositional environments and food supply on energetic tropical shelves (Aller and Stupakoff, 1996, Sumida et al., 2020). Model-based inference further indicates that these biological patterns reflect the combined influence of plume-linked variables (POC and salinity) and background constraints (temperature and depth), highlighting coupled roles of carbon supply and habitat filters in shaping benthic distribution on the Amazon-Guiana margin (Gaurisas and Bernardino, 2023; Gaurisas et al., 2024).

## 4.1 Spatio-temporal POC variability on the Amazon-Guianas shelf

Our study advances understanding of the long-term variability of organic carbon on the Amazon-Guianas shelf by highlighting the influence of a well-defined seasonal hydrological regime, with a biannual oscillation characterized by increased discharge during the rainy season and reduced discharge during the dry season. This pattern is consistent with the precipitation-driven dynamics of large tropical river systems and is aligned with previous studies documenting the strong sensitivity of the Amazon to regional precipitation variability (e.g., Marengo, 2009; Marengo et al., 2016).

The spatial and temporal variability of particulate organic carbon on the Amazonia and Guiana continental shelves is strongly related to the seasonality of the Amazon River flow and the regional circulation patterns of ocean currents, especially the North Brazil Current (Nittrouer and DeMaster, 1996). Although this seasonality has been previously explored, the differences in POC concentrations between groups are also partially explained by the oceanic circulation of the region. The North Brazil Current (NBC) is a surface current that flows through the estuary region, pushing equatorial waters northwesterly (Gouveia et al., 2019). In this sense, much of the freshwater discharged into the ocean by the Amazon estuary is carried northward by the NBC, reducing the POC values below the Amazon River mouth. The freshwater then flows northwestward to the latitude of 7°N, where the NBC retroflection occurs. Further north, the Guiana Current takes over, pushing waters northwestward across the continental shelf (Lumpkin and Garzoli, 2005). After 9°N, POC concentrations are more associated with the outflow of the Orinoco River, which is the fourth largest river in terms of discharge and flows through its delta at latitudes of 9°N and 10°N, carrying its waters by the Guiana Current mainly to the Gulf of Paria, located between 10°N and 11°N on the continental shelf (Gévaudan et al., 2022).

The Mouth and Guiana groups demonstrated a higher dependency on river discharge to achieve higher POC values, likely due to the local circulation that disfavours the supply of continental water in these regions. The north group showed weaker correlation with river discharge, which can be explained by the NBC circulation, which carries fresh water to the region between 3°N and 6°N throughout the year, even in periods of low discharge. The Orinoco group demonstrated a weaker correlation with Amazon River discharge, probably due to its distance from the mouth, added to the local coastal dynamics being much more associated with the outflow of the Orinoco River, carried north by the Guiana Current (López et al., 2012; Gévaudan et al., 2022).

The long-term association between river-ocean dynamics and POC concentrations observed on the Amazon shelf is similar to other large estuaries and deltas globally. In the northeastern continental shelf region of the Gulf of Mexico, POC concentrations from 19 years (2003-2021) of NASA's satellite data showed a strong and positive correlation between POC and Chl-a related to the primary productivity of the region (Ahmad and Jhara, 2025). As observed in the Mexico study, our database on POC productivity is derived from satellite ocean colour data, which may not fully capture the complexities of turbid coastal waters, especially on a short temporal scale, thereby affecting the POC distribution (Ahmad and Jhara, 2025). Although we recognize these limitations, there are no *in-situ* data available for the calibration and validation of decadal ocean productivity from that region.

## 4.2 The Amazon-Guianas shelf benthos distribution

Our analysis of occurrence data revealed high benthic diversity on the Amazon continental shelf, with 4,541 records distributed across 12 phyla, likely reflecting the complex ecological mosaic generated by fluvial, sedimentary, and oceanographic processes. Benthic composition on the region suggests a dynamic sedimentary environment with high productivity. In support of our hypothesis, the composition and structure of benthic communities were spatially heterogeneous, with richness patterns associated with differentiated plume influence. Regions under strong river influence, such as the Mouth and Orinoco, presented greater occurrence totals, whereas species richness remained comparatively high for Cnidaria and Mollusca in Mouth and for Echinodermata in Guiana, showing that frequency and richness do not necessarily covary.

The regional benthic composition may partly reflect the high representativeness of data from fisheries monitoring programs, which often use trawls and traps selectively targeting commercially important crustaceans (Boakes et al., 2010; Costello et al., 2013). However, natural spatial gradients in substrate and biogenic habitat probably also explain regional dissimilarities. In the Mouth region, the high proportion of cnidarian records, especially Hydrozoa and Hexacorallia, is consistent with the presence of consolidated bottoms, rhodolith beds, sponges, and reef habitats associated with the Great Amazon Reef System described for the outer shelf under plume influence (Moura et al., 2016; Francini-Filho et al., 2018). The recent description of hydroids from reef habitats under the Amazon plume further supports the interpretation that hydrozoan records in this sector are linked to structured benthic habitats rather than only to soft-bottom assemblages (Campos et al., 2024).

The grouping of the Guiana and Orinoco regions suggests that these areas share environmental conditions such as greater offshore stability, salinity control, and organic-matter deposition that favour taxa adapted to muddy and mixed bottoms. By contrast, the Mouth region combines intense plume forcing with heterogeneous substrate types, including unconsolidated sediments, carbonate structures, rhodoliths, sponge grounds, and reef patches, which likely contributes to its distinct composition (Francini-Filho et al., 2018). This interpretation also helps explain why Hydrozoa dominated the Mouth sector whereas Anthozoa dominated the northern sectors: hydroids may be favoured by shallow consolidated substrates and by sampling concentrated in near-mouth habitats, whereas octocorals and hexacorals are more frequently reported from outer-shelf and mesophotic reef environments farther north (Gaurisas and Bernardino, 2023; Bernardino et al., 2023). Because the available databases integrate heterogeneous surveys, part of this contrast may still reflect sampling bias, and this caveat should accompany any ecological inference from the regional comparisons.

The spatial distribution of benthic communities observed on the Amazonia and Guiana continental shelves reflects the combined influence of hydrodynamic, sedimentary, and biogeochemical factors associated with particulate organic carbon (POC) supplied by the Amazon River plume. Nevertheless, an important limitation of the present study is that the POC dataset is satellite-derived and therefore represents surface plume conditions, whereas the benthic records are concentrated mostly within the upper 100 m of the shelf. For this reason, our analysis does not resolve plume thickness or the vertical penetration of plume effects across all bathymetric strata; instead, it identifies broad spatial associations between surface plume behaviour and benthic occurrence patterns in the best-sampled shelf domain. These interactions are also relevant from a management perspective because the region is increasingly exposed to anthropogenic pressures, including intense and often weakly regulated fishing activity and the expansion of oil and gas exploration proposals near the Amazon margin, both of which heighten the need for precautionary biodiversity assessment and monitoring.

Our results supports a clear regional structuring of the benthic assemblage, with the Mouth region separating from the more northern sectors and Guiana–North–Orinoco exhibiting greater similarity in relative phylum composition. This pattern is consistent with strong environmental contrasts between the highly turbid, river-proximal shelf and downstream sectors, influenced by varying plume residence times and hydrographic mixing (Nittrouer and DeMaster, 1996; Gévaudan et al., 2022). At the same time, the occurrence totals (bubble sizes) highlight unequal data density among regions, which can arise from spatial biases in biodiversity data collection and reporting (Boakes et al., 2010; Costello et al., 2013; Vandepitte et al., 2015; Zhang and Grassle, 2002).

Random Forest models support benthic assemblages influenced by a combination of plume-related gradients (POC and salinity) and background habitat constraints (temperature and depth). This agrees with expectations that organic-matter supply and particle loads from large rivers interact with shelf circulation and stratification to shape benthic habitat suitability and food availability. The ordination of predictor space (Figure 8b) provides an interpretable summary of these gradients, with PC1 capturing a salinity–temperature axis and PC2 reflecting depth-related variation, thereby offering a mechanistic context for regional clustering of phyla in environmental space (Jolliffe and Cadima, 2016). Because permutation-based importance can be biased under correlated predictors, the relative weights should be interpreted as indicative rather than strictly causal.

In summary, our work reveals an important role of plume dynamics to the Amazon-Guiana benthic shelf distribution with further implications for management and spatial planning. The benthic environment of the Mouth region is governed by stronger sedimentary and turbidity effects, while downstream sectors may experience more stable salinity regimes and different modes of organic enrichment that favour distinct functional assemblages. Such dynamics and sediment-driven stress gradients are classic structuring mechanisms in shelf benthos and can produce strong compositional turnover even at broad taxonomic resolution. Together, these results reinforce that Amazon–Orinoco plume variability is not merely a pelagic feature but a first-order driver of benthic distribution and composition on the North Brazil shelf, acting through coupled carbon supply and hydrographic habitat filtering.

# 5 Conclusions

This study presents a 21-year (2003–2023) assessment of satellite-derived particulate organic carbon (POC) across the

Amazonia–Guiana shelf and demonstrates that POC variability is tightly coupled to Amazon River discharge and strongly mediated by regional circulation. Persistently elevated POC north of the Amazon mouth is consistent with plume advection by the North Brazil Current, whereas comparatively lower values along the Guiana shelf are consistent with offshore export and plume retroflection. Cluster analysis resolved four shelf sectors (Mouth, North, Guiana, and Orinoco) with contrasting long-term mean POC regimes and significant discharge–POC coupling. The benthic database comprised 4,541 records and 12 phyla, dominated by Arthropoda, Cnidaria, Echinodermata, and Mollusca, but with clear regional contrasts in both occurrence structure and species richness. Together, these findings support a mechanism in which river-derived carbon supply interacts with shelf hydrography, substrate heterogeneity, and habitat availability to structure broad-scale benthic distribution patterns across the Amazonia–Guiana margin, while also highlighting the need to account for uneven source datasets and sampling effort in future syntheses.

## Data availability statement

The original contributions presented in the study are included in the article/Supplementary Material. Further inquiries can be directed to the corresponding author.

## Author contributions

AP: Software, Writing – original draft, Investigation, Formal analysis, Data curation, Methodology, Writing – review & editing. AA: Data curation, Methodology, Software, Writing – review & editing, Writing – original draft, Formal analysis. DG: Formal analysis, Writing – review & editing, Investigation, Methodology, Writing – original draft. AB: Writing – original draft, Funding acquisition, Resources, Project administration, Investigation, Validation, Writing – review & editing, Formal analysis, Conceptualization, Supervision, Visualization, Data curation, Methodology, Software.

## Funding

The author(s) declared that financial support was received for this work and/or its publication. We thank FAPES (Fundação de Amparo à Pesquisa e Inovação do Espírito Santo, Brazil) for A. B. A. Postdoctoral fellowship (Profix 2025) and research funding. This work was supported by the PELD Program (PELD-HCES site), funded by Conselho Nacional de Desenvolvimento Científico e Tecnológico (CNPq, grant number 441107/2020) and Fundação de Amparo à Pesquisa do Espírito Santo (FAPES, grant number 186/2021). This is a PELD-HCES contribution #28.

## Conflict of interest

The authors declared that this work was conducted in the absence of any commercial or financial relationships that could be construed as a potential conflict of interest.

## Generative AI statement

The author(s) declared that generative AI was used in the creation of this manuscript. During the preparation of this work the first authors used Chat GPT 5.2 on the manuscript to improve text clarity and fluidity amongst paragraphs. After using this tool/service, the authors reviewed and edited the content as needed and take full responsibility for the content of the publication.

Any alternative text (alt text) provided alongside figures in this article has been generated by Frontiers with the support of artificial intelligence and reasonable efforts have been made to ensure accuracy, including review by the authors wherever possible. If you identify any issues, please contact us.

## Publisher's note



## Supplementary material

The Supplementary Material for this article can be found online at: https://www.frontiersin.org/articles/10.3389/fmars.2026.1805720/full#supplementary-material

## References

Ahmad, H., and Jhara, S. I. (2025). Mapping the dynamics of particulate organic carbon: Satellite observations of coastal to shelf variability in the northeastern Gulf of Mexico. *Ocean Sci. J.* 60, 7. doi: 10.1007/s12601-024-00203-9

Aller, J. Y., and Stupakoff, I. (1996). The distribution and seasonal characteristics of benthic communities on the Amazon shelf as indicators of physical processes. *Cont. Shelf Res.* 16, 717–751. doi: 10.1016/0278-4343(96)88778-4

Apley, D. W., and Zhu, J. (2020). Visualizing the effects of predictor variables in black box supervised learning models. *J. R. Stat. Society: Ser. B. (Stat. Methodol.)* 82, 1059–1086. doi: 10.1111/rssb.12377

Arlot, S., and Celisse, A. (2010). A survey of cross-validation procedures for model selection. *Stat. Surv.* 4, 40–79. doi: 10.1214/09-SS054

Assis, J., Tyberghein, L., Bosch, S., Verbruggen, H., Serrão, E. A., and De Clerck, O. (2018). Bio-ORACLE v2.0: Extending marine data layers for bioclimatic modelling. *Global Ecol. Biogeogr.* 27, 277–284. doi: 10.1111/geb.12693

Bernardino, A. F., Gaurisas, D. Y., and Sumida, P. Y. G. (2023). "Biology, ecology and threats to cold-water corals on Brazil's deep-sea margin," in *Cold-water coral reefs of the world, coral reefs of the world*, vol. 19 . Eds. R. Cordes and F. Mienis Cham, Switzerland: Springer, 31–50. doi: 10.1007/978-3-031-40897-7_2

Bernardino, A. F., Mazzuco, A. C. A., Souza, F. M., Santos, T. M. T., Sanders, C. J., Massone, C. G., et al. (2022). The novel mangrove environment and composition of the Amazon Delta. *Curr. Biol.* 32, 3636–3640. doi: 10.1016/j.Cub.2022.06.071

Boakes, E. H., McGowan, P. J. K., Fuller, R. A., Chang-qing, D., Clark, N. E., O'Connor, K., et al. (2010). Distorted views of biodiversity: Spatial and temporal bias in species occurrence data. *PLoS Biol.* 8, e1000385. doi: 10.1371/journal.pbio.1000385

Bray, J. R., and Curtis, J. T. (1957). An ordination of the upland forest communities of southern Wisconsin. *Ecol. Monogr.* 27, 325–349. doi: 10.2307/1942268

Breiman, L. (2001). Random forests. *Mach. Learn.* 45, 5–32. doi: 10.1023/A:1010933404324

Campos, F. F., de Moura, A. C., de Oliveira Fernandez, M., Marques, A. C., and Pérez, C. D. (2024). Hydroids from a reef system under the influence of the Amazon River plume, Brazil. *Mar. Environ. Res.* 198, 106563. doi: 10.1016/j.marenvres.2024.106563

Clarke, K. R. (1993). Non-parametric multivariate analyses of changes in community structure. *Aust. J. Ecol.* 18, 117–143. doi: 10.1111/j.1442-9993.1993.tb00438.x

Coles, V. J., Brooks, M. T., Hopkins, J., Stukel, M. R., Yager, P. L., and Hood, R. R. (2013). The pathways and properties of the Amazon River plume in the tropical North Atlantic Ocean. *J. Geophys. Res.: Oceans* 118, 6894–6913. doi: 10.1002/2013JC008981

Cordeiro, R. T. S., Neves, B. M., Rosa-Filho, J. S., and Pérez, C. D. (2015). Mesophotic coral ecosystems occur offshore and north of the Amazon River. *Bull. Mar. Sci.* 91, 491–510. doi: 10.5343/bms.2015.1025

Costello, M. J., Michener, W. K., Gahegan, M., Zhang, Z.-Q., and Bourne, P. E. (2013). Biodiversity data should be published, cited, and peer reviewed. *Trends Ecol. Evol.* 28, 454–461. doi: 10.1016/j.tree.2013.05.002

Coynel, A., Seyler, P., Etcheber, H., Meybeck, M., and Orange, D. (2005). Spatial and seasonal dynamics of total suspended sediment and organic carbon species in the Congo River. *Global Biogeochem. Cycles* 19, GB4019. doi: 10.1029/2004GB002335

Dagg, M., Benner, R., Lohrenz, S., and Lawrence, D. (2004). Transformation of dissolved and particulate materials on continental shelves influenced by large rivers: Plume processes. *Cont. Shelf Res.* 24, 833–858. doi: 10.1016/j.csr.2004.02.003

De Pooter, D., Appeltans, W., Bailly, N., Bristol, S., Deneudt, K., Eliezer, M., et al. (2017). Toward a new data standard for combined marine biological and environmental datasets – expanding OBIS beyond species occurrences. *Biodivers. Data J.* 5, e10989. doi: 10.3897/BDJ.5.e10989

Ducklow, H. W., Steinberg, D. K., and Buesseler, K. O. (2001). Upper ocean carbon export and the biological pump. *Oceanography* 14, 50–58. doi: 10.5670/oceanog.2001.06

Feng, L., and Hu, C. (2017). Land adjacency effects on MODIS Aqua top-of-atmosphere radiance in the shortwave infrared: Statistical assessment and correction. *J. Geophys. Res.: Oceans* 122, 4802–4818. doi: 10.1002/2017JC012874

Francini-Filho, R., Asp, N. E., Siegle, E., Hocevar, J., Lowyck, K., D'Avila, N., et al. (2018). Perspectives on the Great Amazon Reef: Extension, biodiversity and threats. *Front. Mar. Sci.* 5. doi: 10.3389/fmars.2018.00142

Friedman, J. H. (2001). Greedy function approximation: A gradient boosting machine. *Ann. Stat.* 29, 1189–1232. doi: 10.1214/aos/1013203451

Garnier, S., Ross, N., Rudis, B., Camargo, A. P., Sciaini, M., and Scherer, C. (2024). viridis(Lite): Colorblind-Friendly Color Maps for R. viridis package version 0.6.5.. doi: 10.32614/CRAN.package.viridis

Gaurisas, D. Y., and Bernardino, A. F. (2023). Benthic biogeographic patterns on the deep Brazilian margin. *PeerJ* 11, e14585. doi: 10.7717/peerj.14585

Gaurisas, D. Y., de Jonge, D. S. W., Sweetman, A. K., and Bernardino, A. F. (2024). Effects of increased temperature and altered POC composition on a bathyal macrofaunal community in Cabo Verde, NE Atlantic. *Prog. Oceanogr.* 229, 103352. doi: 10.1016/j.pocean.2024.103352

Gévaudan, M., Durand, F., and Jouanno, J. (2022). Influence of the Amazon-Orinoco discharge interannual variability on the western tropical Atlantic salinity and temperature. *J. Geophys. Res.: Oceans* 127, e2022JC018495. doi: 10.1029/2022JC018495

Gooday, A. J. (2002). Biological responses to seasonally varying fluxes of organic matter to the ocean floor: A review. *J. Oceanogr.* 58, 305–332. doi: 10.1023/a:1015865826379

Gouveia, N. A., Gherardi, D. F. M., Wagner, F. H., Paes, E. T., Coles, V. J., and Aragão, L. E. O. C. (2019). The salinity structure of the Amazon river plume drives spatiotemporal variation of oceanic primary productivity. *J. Geophys. Res.: Biogeosci.* 124, 147–165. doi: 10.1029/2018JG004665

Greenwell, B. M. (2017). Pdp: An R package for constructing partial dependence plots. *R J.* 9, 421–436. doi: 10.32614/RJ-2017-016

Jolliffe, I. T., and Cadima, J. (2016). Principal component analysis: A review and recent developments. *Philos. Trans. R. Soc. A. Math. Phys. Eng. Sci.* 374, 20150202. doi: 10.1098/rsta.2015.0202

Klautau, A. G. C., Cordeiro, A. P. B., das Chagas, R. A., Santos, W. C. R., Marceniuk, A. P., Vilela da Nóbrega, P. S., et al. (2025). Biodiversity hotspots and threatened species under human influence in the Amazon continental shelf. *Sci. Rep.* 15, 26681. doi: 10.1038/s41598-025-11261-x

Kuhn, M., and Johnson, K. (2019). *Feature engineering and selection: A practical approach for predictive models* (United States: Chapman & Hall/CRC). doi: 10.1201/9781315108230

Lana, P. C., Camargo, M. G., Brogim, R. A., and Isaac, V. J. (1996). *O Bentos da Costa Brasileira: avaliação crítica e levantamento* (Rio de Janeiro, Brazil: FEMAR).

López, R., Del Castillo, C. E., Miller, R. L., Salisbury, J., and Wisser, D. (2012). Examining organic carbon transport by the Orinoco River using SeaWiFS imagery. *J. Geophys. Res.: Oceans* 117, G03022. doi: 10.1029/2012JG001986

Lumpkin, R., and Garzoli, R. (2005). Near-surface circulation in the Tropical Atlantic Ocean. *Deep-Sea Research Part I: Oceanographic Research Papers* 52, 495–518.

Marengo, J. A. (2009). Long-term trends and cycles in the hydrometeorology of the Amazon basin since the late 1920s. *Hydrol. Processes* 23, 3236–3244. doi: 10.1002/hyp.7396

Marengo, J. A., Williams, E. R., Alves, L. M., Soares, W. R., and Rodriguez, D. A. (2016). "Extreme seasonal climate variations in the Amazon Basin: Droughts and floods," in *Interactions between biosphere, atmosphere and human land use in the amazon basin. Ecological studies 227*. Eds. L. Nagy, B. Forsberg and P. Artaxo (Berlin, Heidelberg, Germany: Springer), 99–118. doi: 10.1007/978-3-662-49902-3_4

Molnar, C. (2022). *Interpretable machine learning*. Available online at: https://christophm.github.io/interpretable-ml-book/. (Accessed March 23, 2026).

Moura, R. L., Amado-Filho, G. M., Moraes, F. C., Brasileiro, P. S., Salomon, P. S., Mahiques, M. M., et al. (2016). An extensive reef system at the Amazon River mouth. *Sci. Adv.* 2, e1501252. doi: 10.1126/sciadv.1501252

Nittrouer, C. A., and DeMaster, D. J. (1996). The Amazon shelf setting: Tropical, energetic, and influenced by a large river. *Cont. Shelf Res.* 16, 553–573. doi: 10.1016/0278-4343(95)00069-0

Provoost, P., De Pooter, D., Appeltans, W., Bailly, N., Bristol, S., Deneudt, K., et al. (2017). Expanding the Ocean Biogeographic Information System (OBIS) beyond species occurrences. *Biodivers. Inf. Sci. Stand.* 1, e20515.

QGIS Development Team (2023). *QGIS geographic information system* (Laax, Switzerland: Open Source Geospatial Foundation Project). Available online at: http://qgis.osgeo.org (Accessed March 10, 2026).

Quintana, C. O., Bernardino, A. F., Moraes, P. C., Valdemarsen, T., and Sumida, P. Y. G. (2015). Effects of coastal upwelling on the structure of macrofaunal communities in SE Brazil. *J. Mar. Syst.* 143, 120–129. doi: 10.1016/j.jmarsys.2014.11.003

R Core Team (2024). *R: A language and environment for statistical computing* (Vienna, Austria: R Foundation for Statistical Computing). Available online at: https://www.R-project.org/ (Accessed March 10, 2026).

Richey, J., Hedges, J., Devol, A. H., Quay, P. D., Victoria, R., Martinelli, L., et al. (1990). Biogeochemistry of carbon in the amazon river. *Limnol. Oceanogr.* 35, 352–371. doi: 10.4319/lo.1990.35.2.0352

Richey, J. E., Meade, R. H., Salati, E., Devol, A. H., Nordin, C. F., and Dos Santos, U. (1986). Water discharge and suspended sediment concentrations in the Amazon River: 1982–1984. *Water Resour. Res.* 22, 756–764. doi: 10.1029/WR022i005p00756

Silva, A. L. J. O., Marceniuk, A. P., Santos, G. J. G., Campos, F. F., Gondim, A. I., Klautau, A. G. C. M., et al. (2025). Fisheries bycatch threatens sessile communities of the Great Amazon Reef System. *Estuar. Coast. Shelf Sci.* 319, 109256. doi: 10.1016/j.ecss.2025.109256

Smith, C. R., DeLeo, F. C., Bernardino, A. F., Sweetman, A. K., and Arbizu, P. M. (2008). Abyssal food limitation, ecosystem structure and climate change. *Trends Ecol. Evol.* 23, 518–528. doi: 10.1016/j.tree.2008.05.002

Smith, W. O., and DeMaster, D. J. (1996). Phytoplankton biomass and productivity in the Amazon River plume: Correlation with seasonal river discharge. *Cont. Shelf Res.* 6, 227–244. doi: 10.1016/0278-4343(95)00007-N

Spalding, M. D., Fox, H. E., Allen, G. R., Davidson, N., Ferdaña, Z. A., Finlayson, M., et al. (2007). Marine ecoregions of the world: A bioregionalization of coastal and shelf areas. *BioScience* 57, 573–583. doi: 10.1641/B570707

Stramski, D., Joshi, I., and Reynolds, R. A. (2022). Ocean color algorithms to estimate the concentration of particulate organic carbon in surface waters of the global ocean in support of a long-term data record from multiple satellite missions. *Remote Sens. Environ.* 269, 112776. doi: 10.1016/j.rse.2021.112776

Stramski, D., Reynolds, R. A., Babin, M., Kaczmarek, S., Lewis, M. R., Röttgers, R., et al. (2008). Relationships between the surface concentration of particulate organic carbon and optical properties in the eastern South Pacific and eastern Atlantic Oceans. *Biogeosciences* 5, 171–201. doi: 10.5194/bg-5-171-2008

Strobl, C., Boulesteix, A.-L., Zeileis, A., and Hothorn, T. (2007). Bias in random forest variable importance measures: Illustrations, sources and a solution. *BMC Bioinf.* 8, 25. doi: 10.1186/1471-2105-8-25

Subramaniam, A., Yager, P. L., Carpenter, E. J., Mahaffey, C., Björkman, K., Cooley, S., et al. (2008). Amazon River enhances diazotrophy and carbon sequestration in the tropical North Atlantic Ocean. *Proc. Natl. Acad. Sci.* 105, 10460–10465. doi: 10.1073/pnas.0710279105

Sumida, P. Y. G., De Leo, F. C., and Bernardino, A. F. (2020). "An introduction to the Brazilian deep-sea biodiversity," in *Brazilian deep-sea biodiversity, Brazilian Marine Biodiversity*. Eds. P. Y. G. Sumida, A. F. Bernardino and F. C. De Léo (Springer, Cham). doi: 10.1007/978-3-030-53222-2_1

Suzuki, R., and Shimodaira, H. (2006). Pvclust: An R package for assessing the uncertainty in hierarchical clustering. *Bioinformatics* 22, 1540–1542. doi: 10.1093/bioinformatics/btl117

Utsumi, G. S., He, D., Berelson, W. M., Castelao, R. M., Yager, P. L., and Medeiros, P. M. (2025). Influence of the Amazon River on the composition of particulate organic carbon in the western tropical Atlantic Ocean. *Geochim. Cosmochim. Acta* 389, 84–99. doi: 10.1016/j.gca.2024.09.011

Vandepitte, L., Bosch, S., Tyberghein, L., Waumans, F., Vanhoorne, B., Hernandez, F., et al. (2015). Fishing for data and sorting the catch: Assessing the data quality, completeness and fitness for use of data in marine biogeographic databases. *Database* 2015, bau125. doi: 10.1093/database/bau125

Wang, G., Zhou, W., Cao, W., Yin, J., Yang, Y., Sun, Z., et al. (2011). Variation of particulate organic carbon and its relationship with bio-optical properties during a phytoplankton bloom in the Pearl River estuary. *Mar. pollut. Bull.* 62, 1939–1947. doi: 10.1016/j.marpolbul.2011.07.003

Ward, J. H. (1963). Hierarchical grouping to optimize an objective function. *J. Am. Stat. Assoc.* 58, 236–244. doi: 10.1080/01621459.1963.10500845

Wickham, H. (2011). ggplot2. *WIREs Comput. Stat.* 3, 180–185. doi: 10.1002/wics.147

Wickham, H., Henry, L., and Seidel, D. (2025). *scales: Scale Functions for Visualization. R package version 1.4.0*. Boston, MA, United States: Posit Software, PBC. Available online at: scales.r-lib.org.

Wilkinson, L., and Friendly, M. (2009). The history of the cluster heat map. *Am. Stat.* 63, 179–184. doi: 10.1198/tas.2009.0033

Wright, M. N., and Ziegler, A. (2017). ranger: A fast implementation of random forests for high dimensional data in C++ and R. *J. Stat. Software* 77, 1–17. doi: 10.18637/jss.v077.i01

Zhang, Y., and Grassle, J. F. (2002). A portal for the ocean biogeographic information system. *Oceanolog. Acta* 25, 193–197. doi: 10.1016/S0399-1784(02)01204-5